Advances in Geo-Energy Research

Vol. 2, No. 1, p. 72-85, 2018
www.astp-agr.com

Original article

Characterization of marine-terrigenous transitional Taiyuan formation shale reservoirs in Hedong coal field, China

Kunjie Li[1,2]*, Gang Chen[2,3], Wei Li[2,3], Xinlong Wu[2,3], Jinchong Tan[2,3], Jiangwen Qu[2,3]

[1]*Department of Earth Science and Engineering, Taiyuan University of Technology, Taiyuan 030024, P. R. China*

[2]*Shanxi Provincial Guoxin Energy Development Group Co., Ltd, Taiyuan 030006, P. R. China*

[3]*Shanxi Key Laboratory of Coal and Coal Measures Gas Geology, Taiyuan 030006, P. R. China*

(Received February 5, 2018; revised February 19, 2018; accepted February 20, 2018; available online February 25, 2018)

Citation:
Li, K., Chen, G., Li, W., Wu, X., Tan, J., Qu, J. Characterization of marine-terrigenous transitional Taiyuan formation shale reservoirs in Hedong coal field, China. *Advances in Geo-Energy Research*, 2018, 2(1): 72-85, doi: 10.26804/ager.2018.01.07.

Corresponding author:
*E-mail: marden2008@163.com

Keywords:
Marine-terrigenous transitional shale
Ordos basin
Hedong coal field
formation

Abstract:
To better understand the basic characteristics of Marine-terrigenous Transitional Taiyuan formation shale (TYS) reservoirs in Hedong coal field, a series of reservoir evaluation experiments were conducted on 33 core samples, which were collected from an exploration shale gas well (SL-1). The results show that organic matters in TYS are Type III gas prone kerogen and are in the high-maturity stage with an average R_o value of 1.87% (ranging from 1.71 to 2.10%). The total organic carbon (TOC) is ranging from 0.29% to 11.87% with an average value of 2.91% and gas content is from 0.41 to 2.96 ml/g, which indicates that TYS still has certain hydrocarbon generation potential despite a mass generation of hydrocarbons occurred during the geological history. XRD analysis shows that TYS is composed mainly of quartz minerals and clay minerals with an average brittleness index of 46.5%, which is relatively favorable for hydraulic fracture. Pore size of TYS ranges from a few nanometers to hundreds of nanometers. The permeability is irrelevant with porosity and its values are all lower than 0.1 md. The average value of BET surface area and BJH volumes are 8.57 m^2/g and 1.84 cm^3/100g, respectively. Similar to previous studies, TOC content is a decisive control on gas adsorption capacity in this study.

1. Introduction

With the development of the global economy and increasing demand for energy, many countries pay more and more attention to the exploration and development of unconventional natural gas, including coalbed methane, tight sandstone gas and natural gas hydrate. Shale gas is one of the unconventional sources of natural gas, which is trapped in shale formations with unique characteristics of self-generation and self-storage (Hill et al., 2007; Strapoc et al., 2010). For the low porosity and low permeability, shale gas development has no economic efficiency and is not widely investigated in the past many years (Hill and Nelson, 2000; Jarvie et al., 2011). In recent years, many advanced methods including experimental analysis technology, horizontal well drilling and simultaneous multi-stage as well as repetitive fracturing are used for exploration and development, which made the shale gas resource commercially exploited in North America. Shale gas is changing the supply pattern of energy in the world (Kuuskraa and Stevens, 2009; Wang et al., 2014).

According to the depositional environment, shale rock can be divided into three types, the marine shale, the marine-terrigenous transitional shale and the terrigenous shale. Shale gas research in North America and China focused mainly on the marine shale reservoirs. However, there is almost no research on the marine-terrigenous transitional shale reservoirs, especially on coal measures shale. The marine-terrigenous transitional shales are very different from marine shales in many ways. The organic matters in marine shales, such as marine shale in North America and South China, are mostly type II and type I kerogen. Due to a single stable marine sedimentary environment, shale has a large continuous deposition thickness that can reach tens or even hundreds of meters. Marine shales are rich in carbonate up to 20%, while the clay minerals are relatively low (Zhang et al., 2009; Zou et al., 2010; Chen et al., 2011).

As a marine-terrigenous alternated facies basin, Ordos basin has been reported by the geological surveys that there are a large amount of shale gas resources in multiple sedimentary strata. Especially, the Permo-Carboniferou shale is considered as one of the most attractive shale gas reservoirs with a large

https://doi.org/10.26804/ager.2018.01.07.

thickness, high organic matter abundance, and high maturity (Xiao et al., 2005; Hao SM et al., 2006; Wang and Li, 2011). As one of the six major coal fields of Shanxi province, Hedong coal field is located in the eastern Ordos basin. A considerable amount of researches have been made on exploration and development for coal and coal-bed methane (Wei et al., 1998; Feng et al., 2002; Sheng et al., 2004; Xie et al., 2015; Fu et al., 2016). The shale reservoirs developed well in Hedong coal field and show good gas concentration indicated by past experience in exploration and development of coal and coal-bed methane. The shale gas resources in Hedong coal field are predicated to be approximately 1.43×10^{12} m^3 and the TYS in Daning-Jixian-Xiangning area is regarded as the potential shale gas play according to nationwide survey of shale gas resource potential evaluation and favorable area optimization (2009-2011) by the Ministry of Land and Resources of Oil and Gas Resources Strategic Research Center of China.

However, shale gas exploration in Hedong coal field is just in the very early stage, there is not sufficient detailed data in the literature to describe the features of this marine-continental transitional shale. To reduce exploration risk and increase economic feasibility, it is important to research the properties of shale gas reservoirs and determine the characterization of the shale in Hedong coal field. In this study, we took advantage of shale cores from Taiyuan formation in well SL-1 (Fig. 1) and conduct their geological and geochemical evaluations by petrographical, mineralogical and petrophysical analysis. The thickness, the total organic carbon (TOC) content, thermal maturity, mineralogy, porosity, permeability, gas content, gas adsorption capacity for the TYS were characterized with a series of experimental data. The goal of our understanding is to make an integrated research on the Upper Carboniferous Taiyuan formation shale gas reservoirs in Hedong coal field.

2. Geological setting

Located in the eastern Ordos basin, the Hedong coal field, which is 400 km in length and 60 km in width, covers an area of 17000 km^2 (Fig. 1). Cambrian, Lower Ordovician, Upper Carboniferous, Permian, Mesozoic and Cenozoic are main sedimentary strata deposited on the Pre-Cambrian metamorphic basement in Hedong coal field, among which the Upper Carboniferous Taiyuan formation is an important coal-bearing formation with a thickness of 50-130 m. Taiyuan formation deposits in the marine-terrigenous transitional environment where the coal, shale and sandstone are associated and the shale seams have a stable thickness.

The eastern Ordos basin was subjected to four orogenies after the deposition of the Taiyuan formation: the Indosinian, Early Yanshanian, Middle-Late Yanshanian and Himalayanian successively, and as a result the eastern Ordos basin is a gentle monocline with SW dip direction and an average dip angle of 6.0 degrees (Guo et al., 1998; Li et al., 2010; Zhao et al., 2010). Well SL-1 is a shale gas exploration well drilled in Hedong coal field, the purpose of which is to uncover the shale gas development potential of marine-terrigenous transitional shale seams. The lithological column of the Taiyuan formation in Well SL-1 can be seen in Fig. 2. There are 11 stable shale seams distributing in Tai 1, the Tai 2 and the Tai 3.

3. Samples and experiment methods

3.1 Samples

Based on drilling data, core observation and shale distribution, a total of 33 core samples (SL01-SL33) were taken from 11 shale seams of Taiyuan formation in well SL-1. The locations of these samples are shown in Fig. 2.

In this study, to describe the geochemical and petrophysical characterization of the TYS, total organic carbon (TOC) content, vitrinite reflectance (R_o), kerogen type index (TI), mineralogy (X-ray diffraction, XRD), Hg porosity, BET surface area and BJH volume, gas content, gas adsorption capacity and permeability were determined by a series of experiments. In addition, visual evaluation via thin section, Rock-Eval pyrolysis and scanning electron microscopy (SEM) were also conducted.

3.2 Methods

33 samples were tested for total organic carbon (TOC) with the Eltra CS-800 carbon-sulfur analyzer in line with the state standard of GB/T 19145-2003. The gas content of these same samples were also measured by Chinese National Standard GB/T 19559-2008. The core samples were immediately put into desorption canisters and were taken to laboratory at the reservoir temperature (45°C) for experiment.

Pyrolysis experiment was conducted on 13 samples with a Jinpu OG-2000V on the basis of GB/T 18602-2012. Samples were crushed (0.07 mm-0.15 mm) and 100 g powdered samples were firstly heated to 300°C and remained for 3 mins, then they are continued to be heated to 600°C at 25°C/min. S_1, S_2, S_3 and T_{max} were obtained.

Vitrinite reflectance (R_o) was conducted on 13 samples with Leica DM4500p/DFC450C.

13 powdered samples were analyzed following the petroleum industry standard SY/T 5163-2010 by a Rigaku Smartlab XRD analyzer for the mineralogical composition. The primary minerals such as clay, quartz, feldspar and pyrite were determined.

Porosity was conducted on 13 samples by Hg porosimetry with a QUANTACHROME POREMASTER 33 Mercury Porosimeter. The pressure of Hg was increased from 0 to 235 Mpa at 20°C and the porosity was calculated by the mercury injection data.

Gold V-Sorb 2800TP was used in N_2 adsorption-desorption experiment with the standard GB/T 21650.3-2011. The methods of Barrett-Joyner-Halendar (BJH) and Brunauer-Emmett-Teller (BET) were employed for calculating pore volume and specific surface area, respectively (Barrett et al., 1951; Zhang et al., 2015; Cai et al., 2016). An ULTRA-PERMTM200 permeameter was used to measure the permeability of 13 samples.

Methane adsorption isotherms were determined on 13 samples through a TerraTek-300 at constant temperature (45°C). The Langmuir isotherm method was used to measure the gas

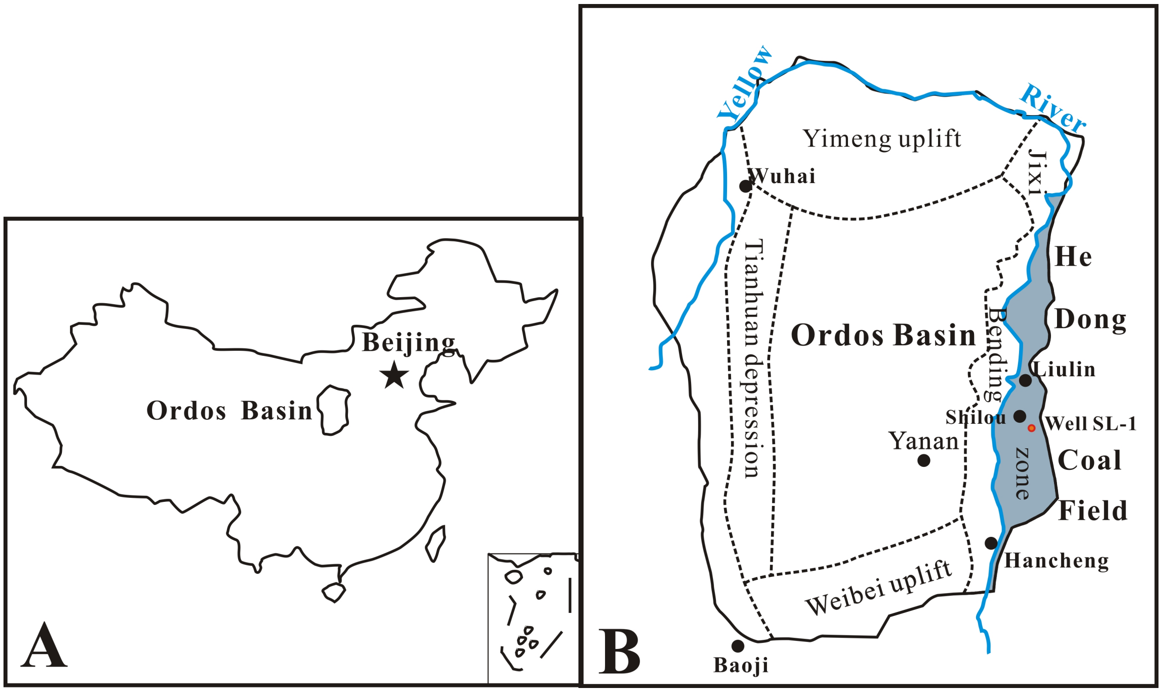

Fig. 1. The location of well SL-1 in Hedong coal field.

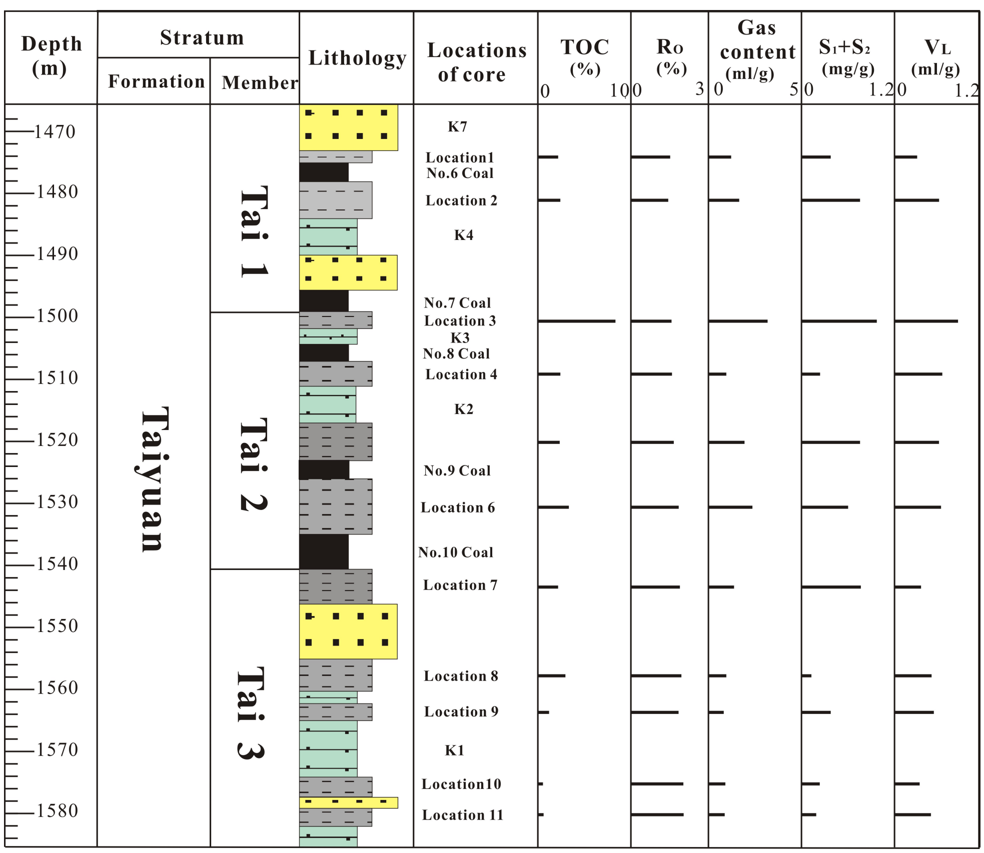

Fig. 2. Lithological column and the locations of the cores in well SL-1.

Table 2. Characteristics of organic matter and gas adsorption capacity for 13 TYS samples.

Samples	R_o (%)	TI	V_L (ml/g)	P_L (Mpa)
SL01	1.71	-71	0.42	0.26
SL04	1.72	-78	0.94	0.35
SL07	1.81	-50	1.02	1.56
SL09	1.84	-83	1.08	0.23
SL10	1.85	-85	0.77	0.46
SL13	1.79	-69	0.33	0.62
SL16	1.86	-76	0.95	0.8
SL20	1.82	-73	0.65	1.14
SL22	1.87	-82	0.45	0.22
SL26	1.94	-81	0.55	1.28
SL28	1.96	-78	0.59	2.03
SL31	2.1	-78	0.39	0.9
SL33	1.94	-76	0.50	0.97

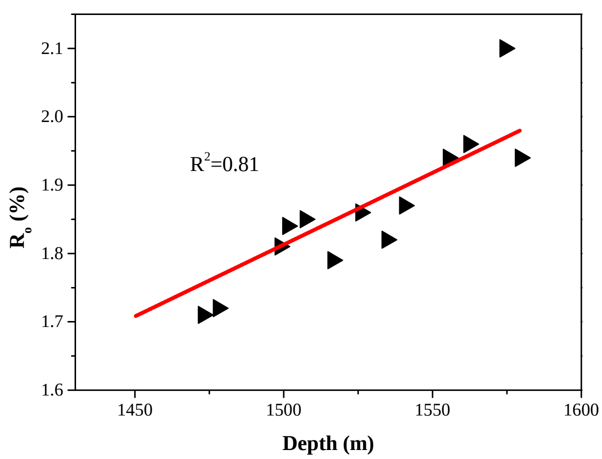

Fig. 3. The relationship between R_o and depth.

absorbed capacity, $V = V_L P/(P_L + P)$, V is the volume of absorbed gas which is the maximum adsorption capacity of the absorbent, V_L represents the Langmuir monolayer volume, P is gas pressure, P_L is the Langmuir pressure, under which the gas adsorption volume (V) equals half of Langmuir volume (V_L) (Langmuir, 1918; Brunauer et al., 1938).

The micropores observation was performed with a Tescan/OXFORD SEM (Abouelresh and Slatt, 2012).

4. Results and discussions

4.1 Depositional environment

According to the characterizations of lithology, fossil flora and abundance of organisms, the Taiyuan formation is regarded as a lagoon-tidal flat depositional system (Jie et al., 2010). The total thickness of the TYS in well SL-1 is 51.84 m, of which Tai 3 is 22.15 m, Tai 2 is 21.79 m, and Tai 1 is 7.90 m. There is no coal seam in Tai 3, and shales in Tai 3 are gray or black. The thickest shale of Tai 3 is 8.29 m. As for Tai 2, it has 3 coal seams and 4 dark grayish black shales which deposit alternately with coal seam as floors or roofs of coal seam. As is shown in Fig. 2, the thickest shale of the Taiyuan formation is 8.90 m in Tai 2. In Tai 1, there are 2 light grayish black shales and 2 thin coal seams.

Single continuous deposition thickness of TYS is thinner than 10 m, which is harmful to development of shale gas in Hedong coal field. Given the TYS deposits with coal seam, sandstone and limestone, scheme of co-exploration and co-development on coal-bed gas, tight sand gas and shale gas in Hedong coal field is an effective way to develop coal measure gas.

4.2 Geochemical Characteristics

Total organic carbon (TOC) contents, vitrinite reflectance values (R_o) and kerogen index (TI) for samples from well SL-1 are presented in table 1 and table 2. TOC of the TYS samples varies from 0.29 to 11.87% with an average of 2.91%. Affected by coal seam, TOC of Tai 2 ranges from 1.90 to 11.87% with a mean value higher than 4.5%, which is greater than Tai 1 (2.35%) and Tai 3 (1.40%). The sample with the largest TOC value (11.87%) is from the floor of number N0. 7 coal in Tai 2. From shale gas exploration and development experience in the United States, only when the TOC concentration is higher than 2%, will shale have a commercial development potential. Thus, Tai 1 has certain resource potential while Tai 2 enjoys a better level (Boker et al, 2007; Jiang et al, 2010).

R_o is a key indicator to assess thermal maturity of organic matter and is correlated with hydrocarbon generation. In general, petroleum generation windows of immature, oil, condensate/wet gas, and dry gas correlate to approximate R_o ranges of 0.5%-0.7%, 0.55%-1.3%, 1.3%-2.0%, and > 2.0%, respectively. R_o value for all TYS samples varies from 1.71% to 2.10% with an average value of 1.87%. It can be seen from Fig. 3 that R_o is increasing with the burial depth as a result of TYS in this area mainly experienced plutonic metamorphism.

Table 1. TOC and gas content for 33 samples from Hedong coal field.

Member	Samples	Depth (m)	TOC (%)	Gas content (cm^3/g)
Tai 1	SL01	1473.0	1.09	1.01
Tai 1	SL02	1473.3	1.12	0.86
Tai 1	SL03	1474.7	4.50	1.56
Tai 1	SL04	1478.0	2.88	1.83
Tai 1	SL05	1480.9	2.65	1.95
Tai 2	SL07	1498.7	11.87	2.96
Tai 2	SL08	1499.0	7.26	2.92
Tai 2	SL09	1450.3	8.34	2.41
Tai 2	SL10	1507.2	3.31	0.98
Tai 2	SL11	1509.2	2.03	1.01
Tai 2	SL12	1510.6	2.01	0.95
Tai 2	SL13	1516.5	0.91	1.01
Tai 2	SL14	1520.0	3.32	1.56
Tai 2	SL15	1522.6	3.00	2.14
Tai 2	SL16	1525.8	6.25	2.91
Tai 2	SL17	1527.1	4.09	2.06
Tai 2	SL18	1528.4	3.79	2.15
Tai 2	SL19	1530.4	3.36	1.86
Tai 2	SL20	1534.6	2.12	0.93
Tai 2	SL21	1534.6	1.90	1.95
Tai 3	SL22	1540.5	2.51	1.79
Tai 3	SL23	1542.2	2.75	0.98
Tai 3	SL24	1544.3	2.07	1.16
Tai 3	SL25	1544.5	1.33	1.05
Tai 3	SL26	1555.2	2.68	1.86
Tai 3	SL27	1555.8	3.33	1.98
Tai 3	SL28	1562.2	0.62	0.65
Tai 3	SL29	1563.3	1.65	1.03
Tai 3	SL30	1564.3	1.35	0.81
Tai 3	SL31	1574.3	0.73	0.71
Tai 3	SL32	1575.0	0.29	0.41
Tai 3	SL33	1579.5	0.61	0.77

The R_o can be directly obtained by testing equipment, it can also be calculated with the method R_o= $0.0180 \times \mathrm{T}_{\max} - 7.16$ as well (Tissot and Welte, 1978; Jarvie and Lundell, 2001). $\mathrm{T}_{\max}$ is the required temperature for kerogen cracking and can be used as an additional chemical assessment to provide conrmation of the visual measurement. When $\mathrm{T}_{\max}$ is from 483.37 °C to 510.09 °C with a mean value of 496.77 °C (table 4), the corresponding R_o is from 1.54 to 2.02%, which is close to but a little less than measured by vitrinite reectance (R_o). Fig. 4 shows that TYS has higher TOC when R_o is between 1.8% and 1.9%, i.e. the burial depth varies from 1495 m to 1540 m.

Normally, organic matter is classified into four types on the basis of macerals: sapropelic (I), humic-sapropelic (II1), sapropelic-humic (II2), and humic (III) (table 4). Visual assessments by the microscope indicate that the kerogen of TYS samples consists mainly of terrestrial organics with a small amount of sapropelic substance (Xiao et al., 2005). The kerogen type index (TI), which is used to decide the kerogen type by counting percentage compositions of different macerals, varies from -50 to -87, with a mean value of -76. The type of organic matter for TYS in Hedong coal field can be determined as typical humic (III), which is in accordance with those previous researches on TYS in eastern Ordos basin.

The kerogen type can also be obtained by the value of HI from the Rock-Eval data. HI represents the amount of thermogenic hydrocarbon in organic matter. The HI values for all samples vary from 11.83 to 36.56 mg/g (table 3), indicating that the kerogen type of TYS from Hedong coal field is type III (table 4), which is in accordance with the result of visual

Table 3. Rock-eval results for 13 TYS samples.

Samples	S_1+S_2 (mg/g)	S_3 (mg/g)	T_{max} (°C)	HI (mg/g)	QI (mg/g)
SL01	0.375	6.402	489.51	32.72	587.29
SL04	0.609	8.210	483.37	20.56	285.07
SL07	1.505	9.955	498.17	12.52	83.87
SL09	1.022	11.729	492.43	11.83	140.64
SL10	0.431	9.180	496.25	12.72	277.34
SL13	0.789	11.213	493.51	23.26	337.75
SL16	0.843	10.770	489.59	13.18	172.32
SL20	0.752	9.801	487.34	34.25	462.32
SL22	0.580	11.324	498.76	22.37	451.14
SL26	0.667	10.845	504.09	24.35	404.65
SL28	0.233	5.402	502.09	36.56	871.21
SL31	0.279	5.309	510.09	35.67	727.27
SL33	0.224	5.031	503.34	36.00	824.77

Table 4. Organic matter type based on the macerals and Rock-eval (Huang et al., 1984).

Kerogen type	Sapropelic (ap)	Humic-sapropelic (μ_1)	Sapropelic-humic (a_2)	Humic (μm)
Maceral of kerogen (TI value)	> 80	40-80	0-40	-120-0
Rock-Eval (HI mg/g)	> 500	350-500	100-350	< 100

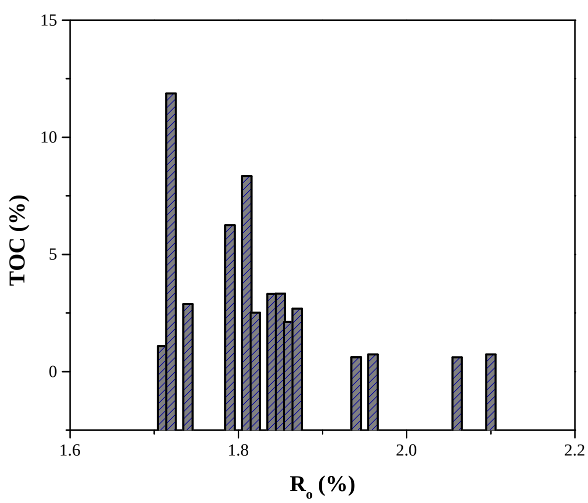

Fig. 4. The plot of TOC vs. R_o.

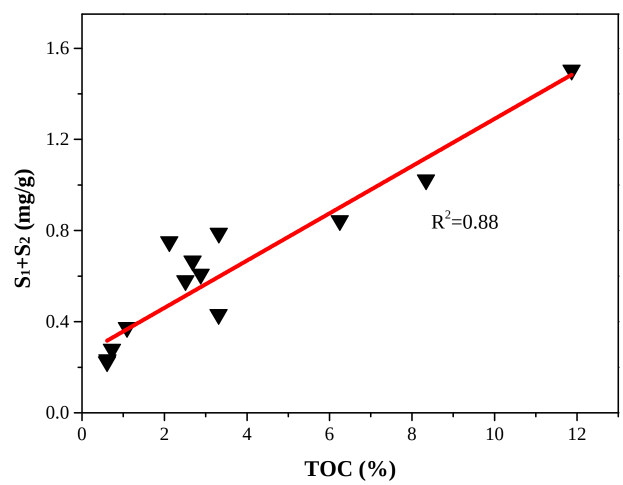

Fig. 5. Relationship between TOC and S_1+S_2.

assessments under the microscope.

The first peak of pyrolysis S_1, which is absorbed on the surface of shale or as free gas exists in the pore of shale, is the amount of volatile hydrocarbon at less than 300°C. S_2 is the amount of pyrolysis compound. S_3 represents the amount of CO_2 generated. As a genetic potential index, S_1+S_2 is used to assess the hydrocarbon-generating potential. Table 3 shows that S_1+S_2 ranges from 0.224 mg/g to 1.505 mg/g (averaging 0.639 mg/g), which has an obviously positive relationship with TOC (Fig. 5). Compared with S_2, S_1 is so small that S_2 plays the decisive role for genetic generation in the TYS.

Based on the values of S_1+S_2, shale can be classified into four grades: better ($>$ 6 mg/g), good (2-6 mg/g), poor (0.5-2 mg/g), not ($<$ 0.5 mg/g). By the standard, TYS from Hedong coal field are the poor kind and possesses very low hydrocarbon-generating potential with the organic matter in a highly mature stage. Although a large amount of oil and gas may have been generated in its geological history, Hunt suggested that large quantities of gas may be still potentially generated from secondary cracking of hydrocarbon in thermally mature reservoir. With the development experience of Barnett shale in Newark East Field as an example, cracking

Table 5. Mineralogical composition of the TYS samples.

Samples	Quartz (%)	Feldspar (%)	Carbonate (%)	Clay (%)	Siderite (%)	Pyrite (%)	Brittleness index (I_B) (%)
SL01	64.1	3.1		32.8			67.2
SL04	56.5	2.0		41.5			58.5
SL07	34.6		4.6	60.8			39.2
SL09	46.5			49.7		3.8	50.3
SL10	36.2	1.4		62.4			37.6
SL13	53.7			46.3			53.7
SL16	50.5		2.8	46.7			53.3
SL20	42.1		7.2	50.7	4.0		51.3
SL22	34.3			65.7			34.3
SL26	54.5			45.5			54.5
SL28	39.6			60.4			39.6
SL31	30.4			70.6			30.1
SL33	35.5			64.5			35.5

gas was considered to be a primary source (Hunt et al., 1996; Jarvie et al., 2007).

With the highly mature organic matter (1.71%< R_o <2.10%), the TYS has evolved into the thermogenic gas and dry gas window. Despite the high maturity of the shale, the TOC contents are still relatively high (> 2.0%). Coal seam is the controlling factor influencing the TOC, which is the uniqueness of TYS from Hedong coal field.

4.3 Mineralogy

Brittleness of shale is a major index in reservoir study which can provide a theoretical basis for hydraulic fracturing. The higher the content of brittle minerals shale has, the easier the crack is caused by hydrofracture which is conductive to shale gas seepage. In general, quartz, feldspar, carbonate and pyrite are regarded as high brittle minerals, while clay minerals are with low brittleness. The brittleness index (I_B) was defined to describe the content of brittle mineral in shale and the brittleness index was determined by the following equation (Chen and Xiao, 2013):

$$I_B = (quartz + feldspar + carbonate + siderite + pyrite)/(quartz + feldspar + carbonate + clay + siderite + pyrite) \times 100\%$$

XRD results of TYS in Hedong coal field are shown in table 5. It can be seen from the data that the primary minerals are clay minerals and quartz as well as a small quantity of feldspar, carbonate, and pyrite. Clay minerals, composed of mainly kaolinite, illite, and a small amount of chlorite, vary from 32.8% to 70.6% (average 53.7%). The contents of quartz are between 30.4% and 64.1% (average 44.5%). Feldspar was found in some TYS samples and its content is less than 5%. The content of carbonate (mainly calcite and dolomite) in TYS samples is no more than 7.5% which is much smaller than the marine shale in North America and in southern China. The fact that pyrite and siderite can be detected in some samples

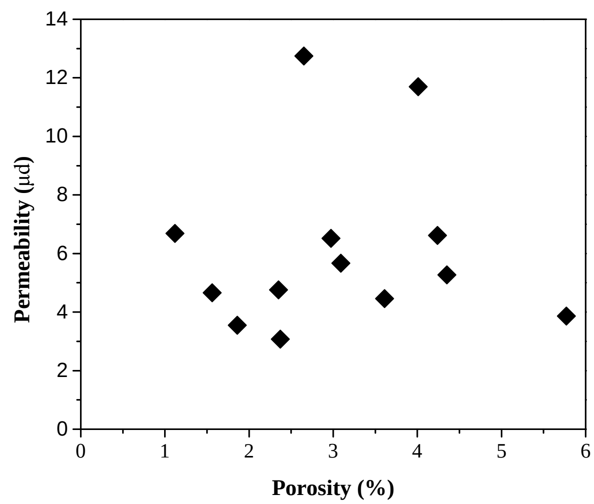

Fig. 6. Plot of porosity vs. permeablity.

(Fig. 6) reveals that TYS was formed in anoxic (reduction) sedimentary environment. The I_B of TYS is from 28.61% to 67.20% with an average value 46.5%, which is adequate for hydraulic fracturing to produce cracks (Based on shale gas E&P experience, the brittle mineral content should be over 40%).

The quartz content and clay mineral content vary in a wide range. The clay minerals are relatively high compared with that of marine shale, while the carbonate content is quite low.

4.4 Porosity and Permeability

According to the International Union of Pure and Applied Chemistry (IUPAC) classification of porous materials, pore can be divided into three types base on pore diameter: micropores (< 2 mm), mesopores (2-50 mm), and macropores (> 50 mm). The macropores give storage room for free gas, while micropores and mesopores can provide a large surface area for

Table 6. Pore characteristics of TYS samples.

Samples	BET surface area (m^2/g)	BJH pore volume (<10 nm) ($cm^3/100g$)	BJH pore volume (<50 nm) ($cm^3/100g$)	BJH pore volume ($cm^3/100g$)	Average pore size (nm)	Hg porosity (%)	Permeability (μd)
SL01	7.00	0.42	1.00	1.59	9.09	4.01	11.70
SL04	12.44	0.73	1.56	2.07	6.64	4.24	6.62
SL07	11.25	1.32	1.89	2.26	7.43	2.65	12.74
SL09	13.56	1.05	2.13	2.90	8.12	3.09	5.67
SL10	8.96	0.78	1.75	2.14	9.57	2.37	3.07
SL13	2.03	0.19	0.64	0.98	26.88	1.97	6.51
SL16	9.32	0.83	1.22	1.81	7.77	5.77	3.86
SL20	7.45	0.47	0.89	1.92	9.31	4.35	5.27
SL22	6.26	0.30	0.82	1.53	9.77	2.35	4.76
SL26	7.89	0.44	0.92	1.49	7.45	3.61	4.46
SL28	7.01	0.41	0.79	1.18	10.73	1.86	3.55
SL31	4.38	0.28	0.68	1.17	11.20	1.12	6.69
SL33	5.06	0.23	0.57	1.23	9.85	1.56	4.66

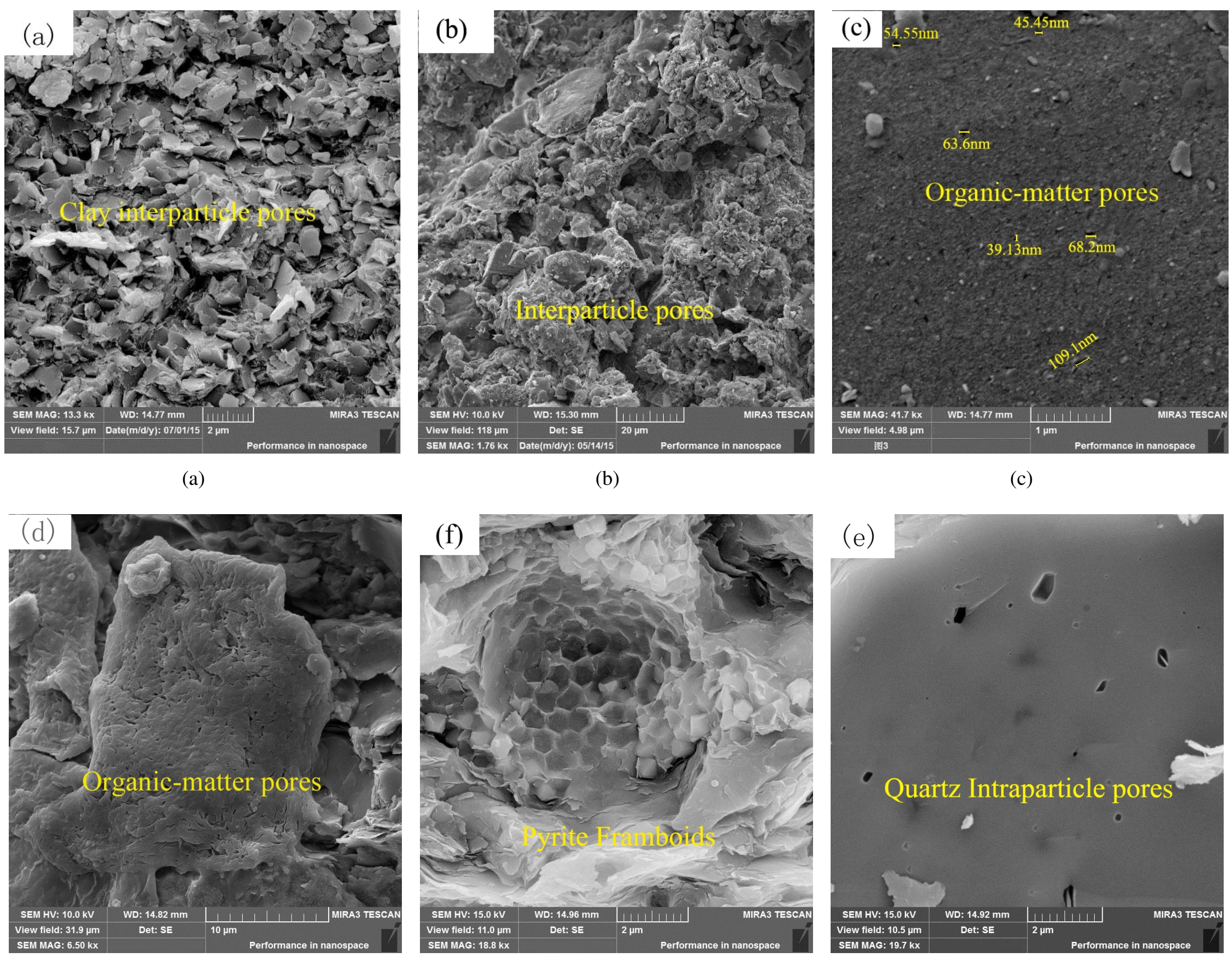

(a) (b) (c)

(d) (e) (f)

Fig. 7. SEM picture of samples: (a) Clay interpartilce pores (SL08); (b) Interparticle pores (SL11); (c) Organic-matter pores (SL09, average<100 nm); (d) Organic-matter pores (SL18); (e) Quartz Intraparticle pores (SL25); (f) Pyrite framboids (SL20).

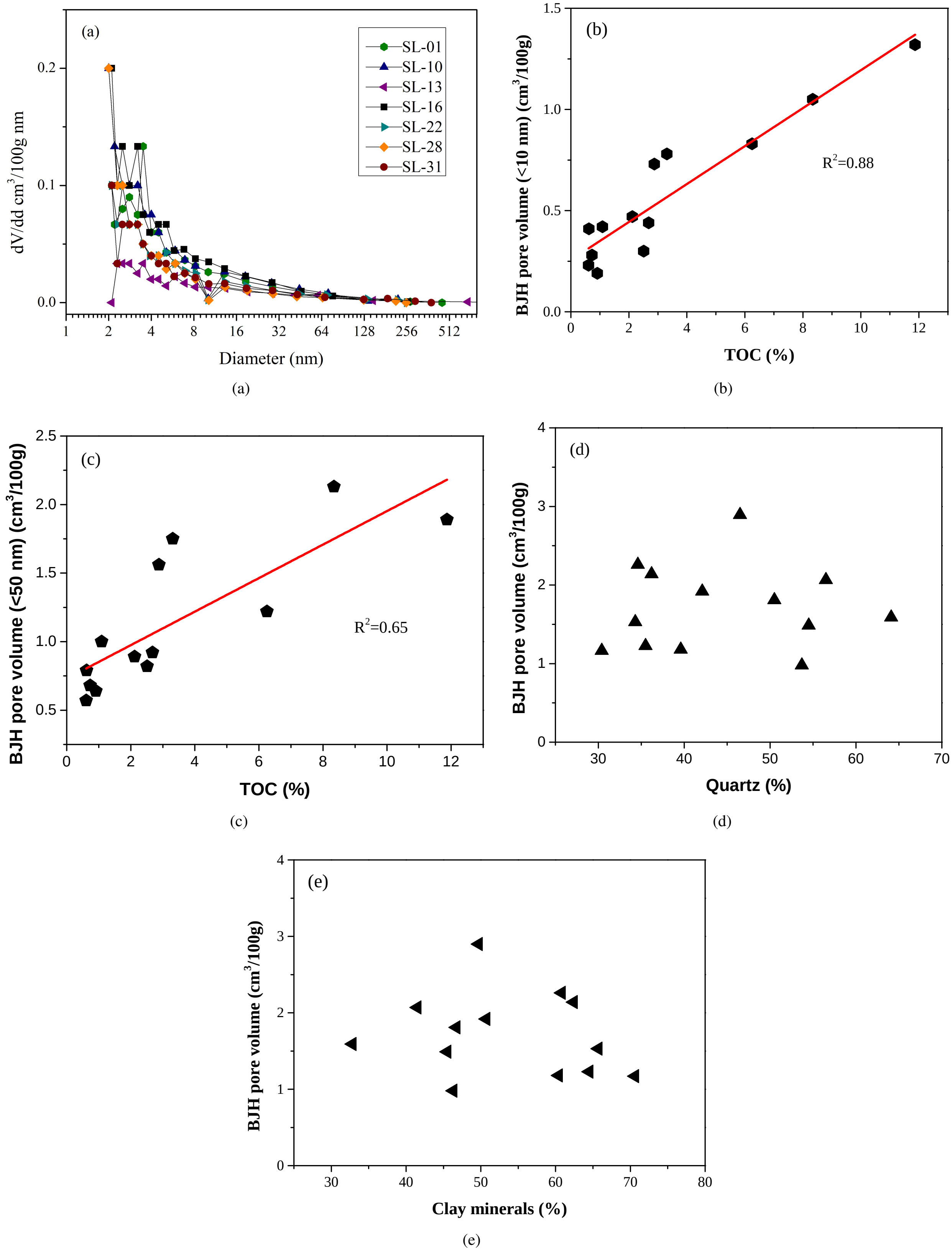

Fig. 8. (a) Plot of pore size distribution for seven samples; the relationships between (b) TOC and BJH pore volume (< 10 nm); (c) TOC and BJH pore volume (< 50 nm); (d) quartz and BJH pore volume; (e) clay minerals and BJH pore volume.

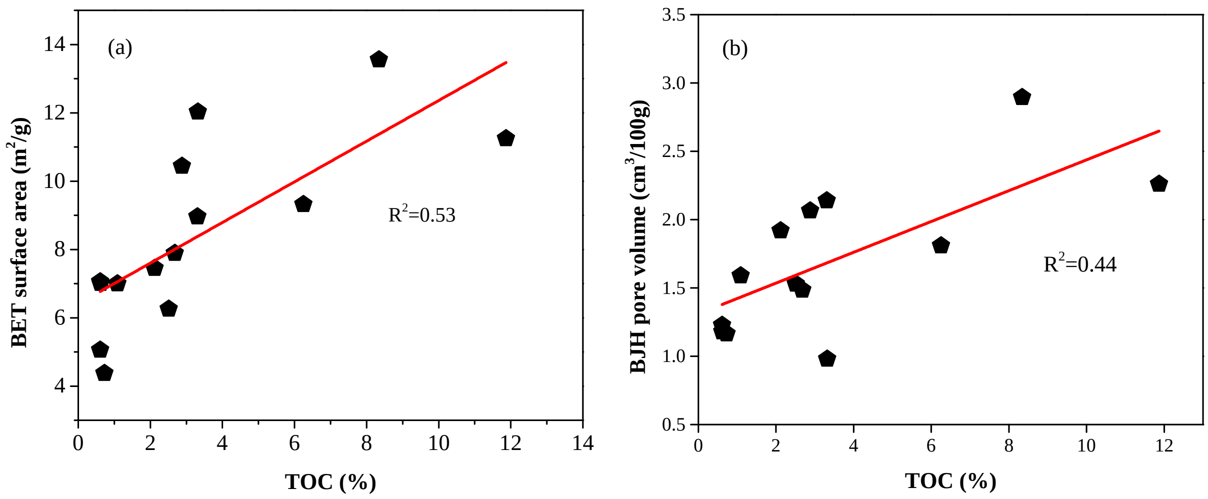

(a) (b)

Fig. 9. The relationships between: (a) TOC and BET surface area; (b) TOC and BJH volume.

adsorbed gas (Rouquerol et al., 1994; Yang et al., 2014). As shown in table 6, the Hg porosity of TYS in Hedong coal field varies between 1.12% and 5.77% with an average of 3.00%. The values of permeability for TYS samples are smaller than 0.1 md (varies from 3.07 to 12.7 μd), indictating that TYS is the ultra-low permeably shale. Although higher porosity is generally associated with the better permeable sediments (Firouzi et al., 2014), there is no correlation between the porosity and permeability, which illustrates the complexity of pore structure in shale (Fig. 6).

Numerous studies have shown that the porosity of shale is significantly affected by mineral compositions. According to the pore occurrence and pore association with mineral particles under SEM, three types of pore are identified in TYS: interparticle pores, intraparticle pores and organic-matter pores (Fig. 7) (Loucks et al., 2012; Wu et al., 2014; Zhang et al. 2016). The SEM evaluation shows that pores in TYS are mainly interparticle pores and organic-matter pores (varying from several nanometers to a few microns), which suggests that mineralogical composition and TOC are the important controlling factors for porosity of the TYS.

The average value of BET surface area for TYS is 7.89 m^2/g (from 2.13 to 13.56 m^2/g). The BJH pore volume is from 1.17 to 2.90 ml/100g with an average of 1.17 $cm^3/100g$. The pore volume with pore size less 10 nm is from 0.19 to 1.32 $cm^3/100g$ and the pore volume with pore size less than 50 nm is from 0.57 to 2.03 $cm^3/100g$. The average pore volume (2.00 $cm^3/100g$) of Tai 2 is higher than that of Tai 1 (1.85 $cm^3/100g$) and Tai 3 (1.32 $cm^3/100g$), which is similar to the Longmaxi shale in Sichuan, China (Nie and Zhang, 2011). Both the BET surface area and the pore volume have an obvious positive relation with TOC (Fig. 9).

The pore size distributions for some samples obtained from low-pressures N_2 adsorption data with BJH model were shown in Fig. 8a. TYS samples have a wide range of PSDs from one or two to hundreds nanometers. Most pores in TYS samples are no more than 50 nm and are mainly less than 10 nanometers. There is a main peak at about 2 nm for many TYS samples and other peaks are between 3 and 4 nm. As the table 6 showed that the pore volume (less than 10 nm) and the pore volume (less than 50 nm) account for the BJH pore volume of 30% and 65%, respectively. The pore size of TYS calculated by the BJH model is between 6.64 nm and 26.88 nm with a mean value of 10.29 nm.

The pores formation and development in shale are mainly affected by the minerals composition and TOC. As the Fig. 8b, 8c showed that TOC has an obvious positive relationship with BJH pore volume ($<$ 10 nm) (Fig. 8b), a moderate positive relationship with BJH pore volume ($<$ 50 nm) (Fig. 8c), and a weak positive correlation with total BJH pore volume(Fig. 9). These relationships indicate that TOC is favorable for micropores development. Due to deposition in the same sedimentary environment, the shale from coal-bearing stratum has same sediment source with coal. Organic matters in TYS samples are also same with coal, which are classified as type III kerogen. TYS also undergoes stages of sedimentation and deterioration, such as stages of peat, lignite, bituminous coal and anthracite. The organic matters in TYS also have macromolecular structure in high maturity or over maturity stage. This macromolecular is constructed of a series of aromatic cores with varying amounts of aliphatic side-chains or functional groups. During diagnosis of coal-shale, the aromatic cores in organic matters are continuously condensed into a larger macromolecular. The result is that hydrogen gas expelled from the organic matters and various shapes of nano-scale pores, mainly micorpores, are produced. The R_o for the TYS is between 1.71% and 2.10%, which is the peak of gas generation for type III kerogen.

As the main mineral component of TYS samples, neither quartz nor clay minerals have determined relationships with BJH pore volume (Figs. 8d and 8e), which indicates that mineral compositions play a complex role in the formation and development of pores in TYS samples.

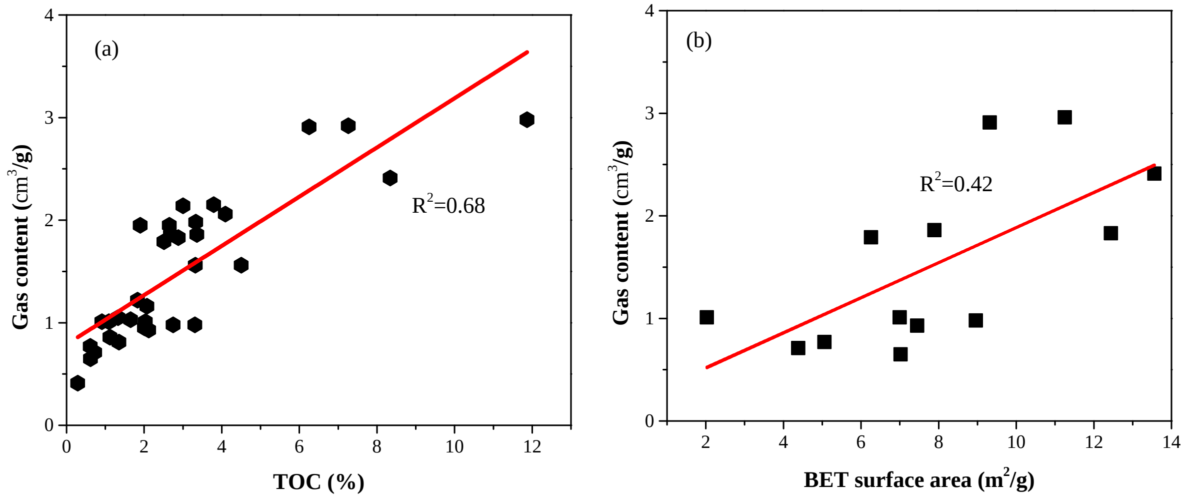

(a) (b)

Fig. 10. The relationships between: (a) TOC and gas content; (b) gas content and BET surface area.

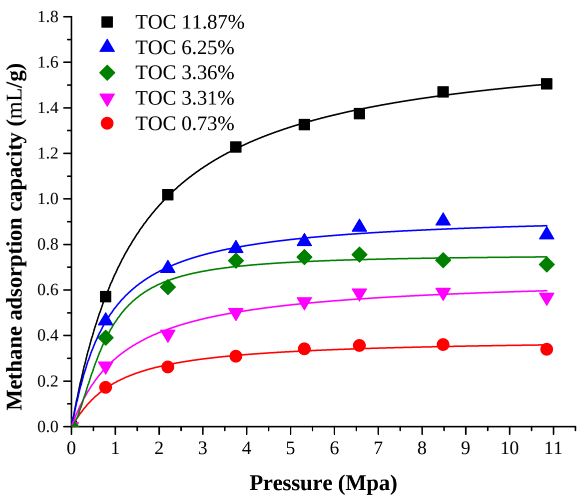

Fig. 11. Methane adsorption isotherms for five core samples with different TOC contents.

4.5 Gas content and methane adsorption capacity

As a self-contained source system, abundant gas can be stored in pores and natural fractures, adsorbed on the organic matter and mineral surface or dissolved in kerogen and bitumen. The gas content, which can be acquired by measuring the gas released from core samples, is used as a key index to determine whether it has economic benefits or has a resource potential (Tang et al., 2011).

The results for gas content tests of TYS in Hedong coal field are summarized in table 1. The values of gas content vary from 0.41 to 2.96 ml/g (1.52 ml/g on average) and the values of the Tai 2 are from 0.93 ml/g to 2.96 ml/g and more than 50% samples are higher than 2.00 ml/g. As the marine-terrigenous transitional shale, the TYS in Hedong coal field has a high gas concentration, especially the samples from Tai 2. Both TOC content and specific surface area have a positive correlation with gas content (Fig. 10). High TOC value is conductive for hydrogen generation and development of micro-pores or nano-scale pores, which can provide enough storage space for shale gas accumulation.

In this work, the methane adsorption was conducted on air dry shale powders under the reservoir temperature (45°C) (Fig. 11). It can be seen in table 2, the V_L was between 0.39 ml/g and 1.72 ml/g, averaged 0.73 ml/g. Compared with the methane adsorption capacity of the Low Cambrian shale from Sichuan basin (2.8 ml/g on average) and northwest Guizhou province (2.28 ml/g on average) (Clarkson et al., 2013; Zhang et al., 2016), the value of TYS is lower without considering experiment condition and moisture content of samples.

Many previous studies have reported that the methane adsorption capacity is closely related to organic matter content, it is also true of TYS samples from Hedong coal field. As Fig. 11 and Fig. 12a illustrated, the values of V_L have a strong positive correlation with TOC content and the large gas adsorption capacity is generally associated with the organic-rich samples (Ross and Bustin, 2007; Ross and Bustin, 2008; Clarkson et al., 2012).

It is thought that the methane adsorption capacity of shale is also dependent on mineral components and there was a positive relationship between the gas sorption capacity and the clay minerals. However, clay minerals have a unique relationship with Langmuir volume V_L in this study. As shown in Fig. 12b, the clay content relates positively with V_L when its value is less than 50% and has a negative association when the value of clay content ranges from 55% to 70%. The clay minerals, especially illite, can provide huge surface area and have great sorption energy which contributes to the gas adsorption. So V_L rises with the clay content increasing when clay minerals are in a certain range. As the clay contents ascend further, the TOC content and brittle minerals are correspondingly decreasing. Clay minerals may fill the micorpores and absorb more moisture since the clay minerals in TYS are very tiny, which is unfavorable for methane sorption, thus, the

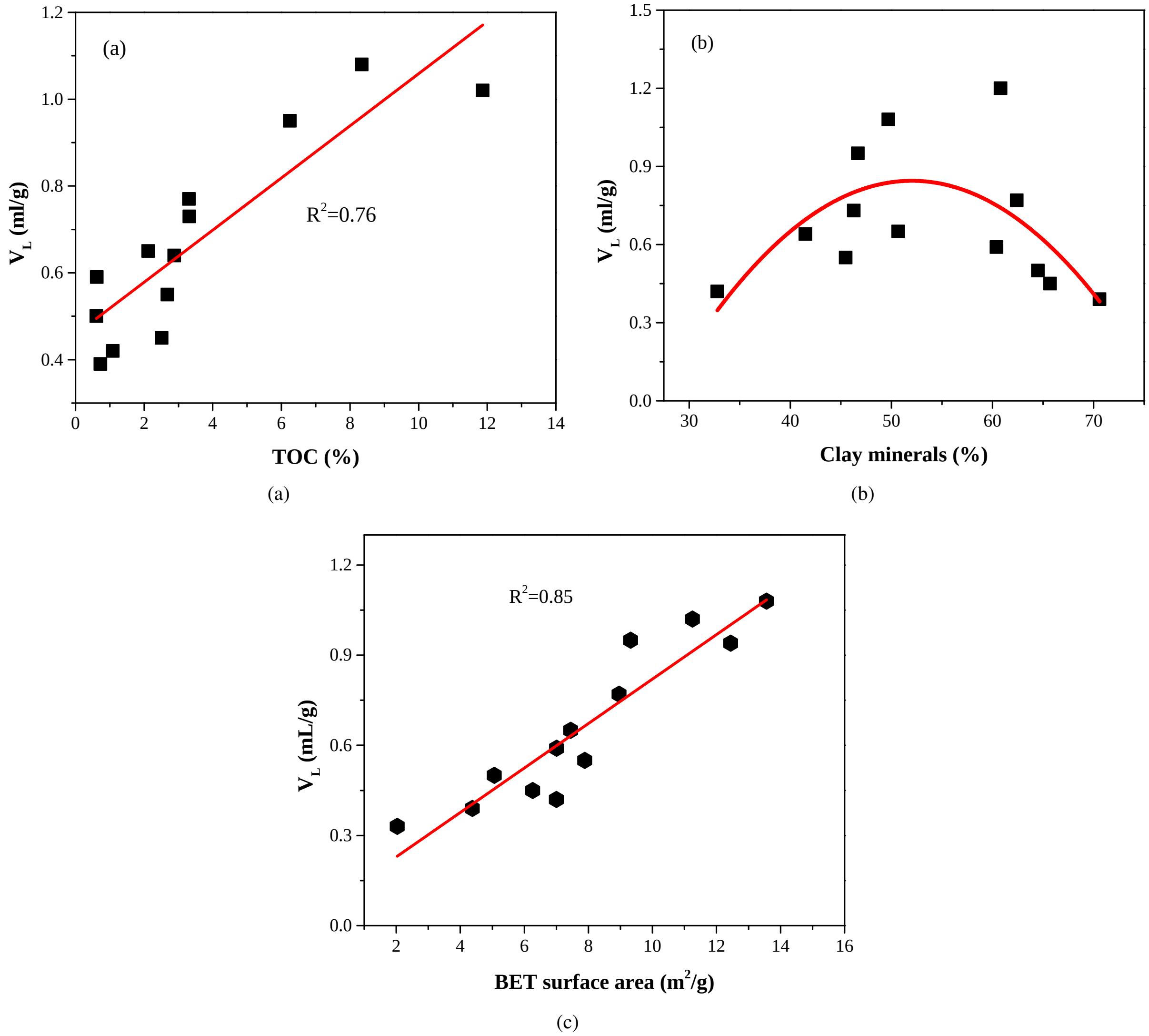

Fig. 12. Correlation plots between: (a) TOC and gas sorption capacity (VL); (b) clay and BET surface area; (c) BET surface area and VL.

gas sorption capacity decreases as the value of clay content is above 55%. Theoretically, the clay minerals have positive effects on methane sorption capacity, but other factors such as TOC, moisture content, pores, etc. affect also the gas sorption capacity. Therefore, there are a variety of relationships between clay minerals and gas sorption capacity in reality (Lu et al., 1995; Clarkson et al., 2012; Ji et al., 2012). A good correlation between BET surface area and V_L is shown in Fig. 12. The V_L increases with the increasing BET surface area. Greater BET surface area can provide more space for adsorbed gas.

5. Conclusions

As the Marine-terrigenous Transitional shale, TYS samples from Hedong coal field has the following characteristics:

(1) The kerogen type of organic matters in TYS samples is humic (III), which is different from the organic matters in marine shale (type I or type II) in North America and south China and is more conducive to the generation of dry gas. Although organic matters has entered a high or over mature stage (R_o from 1.71% to 2.10%), the TOC is still relatively high (ranging from 0.29% to 11.87%).

(2) The mineral composition is characterized by high clay minerals, low carbonate and feldspar. Carbonates in TYS are less than 5% on average, which is far below marine shale (the maximum can reach 20%). As a marker of weak reduction environment, pyrite is also found in some TYS samples.

(3) The PSDs of TYS samples has a wide range of pore size from 2 to hundred nanometers. The dominate pore size is between 2 and 10 nm, which accounts for 30% of BJH pore volume. TOC is a key control factor for pore development of TYS samples, especially for pores less than 10 nm. The permeability of TYS samples is between 3.05 and 12.74 μd, indicating the TYS are ultralow permeability reservoirs. The correlation analysis showed that permeability has no obvious relationship with porosity.

(4) The gas content of TYS is 1.52 ml/g on average (ranging from 0.41 to 2.96 ml/g). Meanwhile, the Langmuir value V_L ranges from 0.33 to 1.08 ml/g (0.66 ml/g on average)

which has a positive correlation with BET surface and TOC content.

Previous studies reported that there is an abundance of coal measure gas including coal-bed methane, sandstone gas in Hedong coal field. It may be unfavorable for shale gas development separately as a result of small single layer thickness (the largest < 10 m). However, it will have a great potential to co-explore and co-develop the coal measures gas in view of the fact that the TYS deposited with coal seam, tight sand stone and even thin limestone.

Acknowledgments

This study is supported by Key Project of Coal-based Science and Technology in Shanxi Province (Grant No. MQ 2014-01) and the project of Shanxi Provincial Shale Gas Resources Investigation and Evaluation Program. The authors also would like to appreciate all anonymous reviewers.

Declaration of conflicting interests

The authors declare no competing nancial interest.

References

Barrett, E.P., Johner, L.S., Halenda, P.P. The determination of pore volume and area distributions in porous substances. I. computations from nitrogen isotherms. J. Am. Chem. Soc. 1951, 73(7): 373-380.

Bowker, K.A. Barnett Shale gas production, Fort Worth Basin: Issues and discussion. AAPG Bull. 2007, 91(4): 523-533.

Brunauer, S., Emmett, P.H., Teller, E. Adsorption of gases in multimolecular layers. J. Am. Chem. Soc. 1938, 60(2): 309-319.

Cai, S.H., Liu, H.Q., He, S.L., et al. Shale reservoir characteristics and exploration potential in the target: A case study in the Longmaxi Formation from the southern Sichuan Basin of China. J. Nat. Gas Sci. Eng. 2016, 31: 86-97.

Chen, S.B., Zhu, Y.M., Wang, H.Y., et al. Shale gas reservoir characterization: a typical case in the southern Sichuan Basin of China. Energy 2011, 36(11): 6609-6616.

Clarkson, C.R., Freeman, M., He, L., et al. Characterization of tight gas reservoir pore structure using USANS/SANS and gas adsorption analysis. Fuel 2012, 95: 371-385.

Clarkson, C.R., Jensen, J.L., Pedersen, P.K., et al. Innovative methods for flow-unit and pore-structure analyses in a tight siltstone and shale gas reservoir. AAPG Bull. 2012, 96(2): 355-374.

Clarkson, C.R., Solano, N., Bustin, R.M., et al. Pore structure characterization of North American shale gas reservoirs using USANS/SANS, gas adsorption, and mercury intrusion. Fuel 2013, 103: 608-616.

Curtis, J.B. Fractured shale-gas systems. AAPG Bull. 2002, 86(11): 1921-1938.

Feng, S.A., Ye, S.L., Zhang, J.P. Coalbed methane resources in the Ordos basin and its development potential. Regional Geology of China 2002, 21(10): 658-662.

Firouzi, M., Rupp, E.C., Liu, C.W. Molecular simulation and experimental characterization of the nanoporous structures of coal and gas shale. Int. J. Coal Geol. 2014, 121: 123-128.

Fu, X.H., Deleqiati, J., Zhu, Y.N., et al. Research characteristics and separated reservoirs' drainage of unconventional gas in coal measures. Earth Science Frontiers 2016, 23(3): 36-40. (In Chinese)

Guo, Y.H., Liu, H.J., Quan, B., et al. Late paleozoic sedimentary system and paleogeographic evolution of Ordos area. Acta Sedimentalogica Senic. 1998, 16(3): 44-51. (In Chinese)

Hao, S.M., Hui, K.Y., Li, L. Reservoir features of Daniudi low-permeability gas field in Ordos basin and its exploration and development technologies. Oil & Gas Geology 2006, 27(6): 762-768.

Hill, D.G., Nelson, C.R. Reservoir properties of the Upper Cretaceous Lewis Shale, a new natural gas play in the San Juan Basin. AAPG Bull. 2000, 84(8): 1240.

Hill, R.J., Jarvie, D.M., Zumberge, J., et al. Oil and gas geochemistry and petroleum systems of the Fort Worth Basin. AAPG Bull. 2007, 91(4): 445-473.

Huang, D.F., Li, J.C., Zhang, D.J. Kerogen types and study on effectiveness limitation and interrelation of their identification parameters. Acta Sedimentalogica Senic. 1984, 2(3): 18-33. (In Chinese)

Hunt, J.M. Petroleum Geochemistry and Geology. Freeman and Company, New York, 1996.

Jarvie, D.M., Hill, R.J., Ruble, T.E., et al. Unconventional shale-gas systems: The Mississippian Barnett Shale of north-central Texas as one model for thermogenic shale-gas assessment. AAPG Bull. 2007, 91(4): 475-499.

Jarvie, D.M., Lundell, L.L. Kerogen type and thermal transformation of organic matter in the Miocene Monterey Formation, The Monterey Formation: From Rocks to Molecules, edited by Isaacs, C.M. and Rullkötter, J., Columbia University Press, New York, pp. 268-295, 2001.

Jiang, Y.Q., Dong, D.Z., Qi, L. Basic features and evaluation of shale gas reservoirs. Natural Gas Industry 2010, 30(10): 7-12. (In Chinese)

Jie, M.X. Prospects in coalbed methane gas exploration and development in the eastern Ordos Basin. Natural Gas Industry 2010, 30(6): 1-6. (In Chinese)

Ji, L.M., Zhang, T.W., Milliken, K.L. Experimental investigation of main controls to methane adsorption in clay-rich rocks. Appl. Geochem. 2012, 27(12): 2533-2545.

Langmuir, I. The adsorption of gases on plane surfaces of glass, mica and platinum. J. Amer. Chem. Soc. 1918, 40(9): 1351-1403.

Li, S.X., Deng, X.Q., Pang, J.L., et al. Relationship between petroleum accumulation of mesozoic and tectonic movement in Ordos basin. Acta Sedimentalogica Senic. 2010, 28(4): 798-807.

Loucks, R.G., Reed, R.M., Ruppel, S.C., et al. Spectrum of pore types and networks in mudrocks and a descriptive classification for matrix-related mudrock pores. AAPG Bull. 2012, 96(6): 1071-1098.

Lu, X.C., Li, F.C., Watson, A.T. Adsorption studies of natural gas storage in Devonian shales. SPE Form. Eval. 1995, 10(2): 109-113.

Montgomery, S.L., Jarvie, D.M., Bowker, K.A., et al. Mississippian Barnett Shale, Fort Worth basin, north-central Texas: Gas-shale play with multitrillion cubic foot potential. AAPG Bull. 2005, 89(2): 155-157.

Nie, H.K., Zhang, J.C. Types and characteristics of shale gas reservoir: A case study of Lower Paleozoic in and around Sichuan Basin. Petroleum Geology and Experiment 2011, 33(3): 219-225. (In Chinese)

Peltonen, C., Marcussen, *Φ*., Bj*ϕ*rlykke, K., et al. Clay mineral diagenesis and quartz cementation in mudstones: The effects of smectite to illite reaction on rock properties. Mar. Pet. Geol. 2009, 26(6): 887-898.

Ross, D.J.H., Bustin, R.M. Shale gas potential of the lower jurassic gordondale member, northeastern British Columbia, Canada. B. Can. Petrol. Geol. 2007, 55(1): 55-75.

Ross, D.J.H., Bustin, R.M. Characterizing the shale gas resource potential of Devonian-Mississippian strata in the Western Canada sedimentary basin: Application of an integrated formation evaluation. AAPG Bull. 2008, 92: 87-125.

Ross, D.J.K., Bustin, R.M. The importance of shale composition and pore structure upon gas storage potential of shale gas reservoirs. Mar. Pet. Geol. 2009, 26(6): 916-927.

Rouquerol, J., Avnir, D., Fairbridge, C.W., et al. Recommendations for the characterization of porous solids (Technical Report). Pure Appl. Chem. 1994, 66(8): 1739-1758.

Strapoc, D., Mastalerz, M., Schimmelmann, A., et al. Geochemical constraints on the origin and volume of gas in the New Albany Shale (Devonian-Mississippian), eastern Illinois Basin. AAPG Bull. 2010, 94(11): 1713-1740.

Tang, Y., Zhang, J.C., Liu, Z.J., et al. Use and improvement of the desorption method in shale gas content tests. Natural Gas Industry 2011, 31(10): 108-112. (In Chicness)

Tissot, B.P., Welte, D.H. Petroleum formation and occurrence: A new approach to oil and gas exploration. Springer, Berlin, 1978.

Wang, C.C., Juang, L.C., Lee, C.K., et al. Effects of exchanged surfactant cations on the pore structure and adsorption characteristics of montmorillonite. J. Colloid Interface Sci. 2004, 280(1): 27-35.

Wang, Q., Chen, X., Jha, A.N., et al. Natural gas from shale formation-The evolution, evidence and challenges of shale gas revolution in the United States. Renew. Sust. Energ. Rev. 2014, 30: 1-28.

Wang, S.J., Li, D.H. Exploration potential of shale gas in the Ordos Basin. Natural Gas Industry 2011, 31(12): 40-46.

Wang, S.W., Duan, L.X., Cheng, Z.H., et al. Reservoir Evaluation for Exploration and development of Coal-bed Gas. Natural Gas Industry 2004, 24: 82-84. (In Chicness)

Warlick, D. Gas shale and CBM development in North America. Oil & Gas J. 2006, 3(11): 1-5.

Wei, C., Sang, S., Liu, H., et al. Coalbed gas geological characters in the middle and south part of Hedong Coal field and their exploration and exploitation future. Geol. Miner. Res. North China 1998, 13: 243-248.

Wu, Y., Fan, T.L., Zhang, J.C., et al. Characterization of the upper Ordovician and lower Silurian marine shale in northwestern Guizhou province of the upper Yangtze block, south China: implication for shale gas potential. Energy fuel 2014, 28(6): 3679-3687.

Xiao, X.M., Zhao, B.Q., Thu, Z.L., et al. Upper Paleozoic petroleum system, Ordos Basin, China. Mar. Pet. Geol. 2005, 22(8): 945-963.

Xie, Y.G,, Meng, S.Z., Wan, H. Analysis on geological conditions of multi-type natural gas reservoir in coal measure strata of Linxing Area. Coal Science and Technology 2015, 43(9): 71-75.

Yang, F., Ning, Z.F., Liu, H.Q. Fractal characteristics of shales from a shale gas reservoir in the Sichuan Basin, China. Fuel 2014, 115: 378-384.

Zhang, J.C., Jiang, S.L., Tang, X., et al. Accumulation types and resources characteristics of shale gas in China. Natural Gas Industry 2009, 29(12): 109-114.

Zhang, J.P., Fan, T.L., Li, J., et al. Characterization of the Lower Cambrian Shale in the Northwestern Guizhou Province, South China: Implications for Shale-Gas Potential. Energy Fuel 2015, 29(10): 6383-6393.

Zhang, Q., Liu, R.H., Pang, Z.L., et al. Characterization of microscopic pore structures in Lower Silurian black shale (S1l), southeastern Chongqing, China. Mar. Pet. Geol. 2016, 71: 250-259.

Zou, C.N., Dong, D.Z., Wang, S.J., et al. Geological characteristics and resource potential of shale gas in China. Petrol. Exolor. Dev. 2010, 37(6): 641-653.